JOURNAL OF APPLIED ELECTROCHEMISTRY 26 (1996) 953–958

Investigation of the hydrogen evolution reaction at a 10 wt % palladium-dispersed carbon electrode using electrochemical impedance spectroscopy

S.-I. PYUN*, T.-H. YANG

Department of Materials Science and Engineering, Korea Advanced Institute of Science and Technology, 373-1 Kusong Dong, Yusong-Gu, Daejon, 305-701, Korea

C.-S. KIM

Fuel Cell Research Team, Korea Institute of Energy Research, PO Box 103, Yusong-Gu, Daejon, 305-343, Korea

Received 7 November 1995; revised 16 January 1996

The hydrogen evolution reaction (h.e.r.) at a 10 wt % palladium-dispersed carbon (Pd/C) electrode in 0.1 M NaOH solution has been investigated with reference to that on carbon (Vulcan XC-72) and palladium foil electrodes by analysing the a.c.-impedance spectra combined with cyclic voltammograms. From the coincidence of the maximum charge transfer resistances and the minimum hydrogen evolution resistances for the h.e.r. at the respective electrode potential for the Pd/C, carbon and Pd foil electrodes, it is suggested that the h.e.r. at the Pd/C electrode takes place along with the absorption and diffusion of hydrogen above −1.10 V vs SCE, whereas the former dominates over the latter below −1.10 V vs SCE. In the case of the Pd foil electrode the transition of absorption and diffusion to evolution occurs at −0.96 V vs SCE. In contrast to the Pd/C and Pd foil electrodes the h.e.r. occurs strongly at the carbon electrode below −1.20 V vs SCE. The hydrogen evolution overpotential on the Pd/C electrode is decreased by 0.10 V in comparison to the carbon electrode due to the larger electrochemical active area of the finely dispersed Pd particles.

1. Introduction

The hydrogen evolution reaction (h.e.r.) at the electrode/electrolyte interface has been widely investigated [1–3]. The mechanism of the h.e.r. in aqueous solution involves the formation of an adsorbed hydrogen atom intermediate (Volmer adsorption), the electrochemical desorption of hydrogen into solution (Heyrovsky desorption) and the chemical desorption by the combination of two adatoms (Tafel desorption) [1–3].

High surface area electrocatalytic electrodes such as Pt, Pd and Ni alloys are of interest for h.e.r. The high surface electrocatalyst can be made by sintering or electrodeposition [4, 5] or by dispersion of an active electrocatalytic material on the electrocatalyst support with a relatively large surface area.

It is reported in recent papers [6–8] that the h.e.r. on a Pd foil electrode is accompanied by absorption and diffusion of hydrogen into the Pd foil. However, in the case of Pd dispersed on an electrocatalyst support, the kinetics of the h.e.r. are promoted or inhibited depending upon the amount and extent of the dispersion of Pd in the electrode.

This work is aimed at investigating the h.e.r. on a 10 wt % Pd–dispersed carbon (Pd/C) electrode in 0.1 M NaOH solution with reference to carbon (Vulcan XC-72) and Pd foil electrodes. For this purpose, a.c.-impedance measurements supplemented by cyclic voltammetry were carried out on the three kinds of electrodes. The complex nonlinear least squares (CNLS) data-fitting method was employed to determine such kinetic parameters as double layer capacitance, charge transfer resistance and hydrogen evolution resistance as a function of the electrode potential.

2. Experimental details

A Pd foil (Aldrich Chemicals) was used as the Pd electrode. The carbon electrode was made of Vulcan XC-72 (Cabot) carbon powders employing the same fabrication process as for the 10 wt % Pd/C electrode. The 10 wt % Pd/C electrode specimen was prepared as follows. 10 wt % Pd/C powder (E-TEK Co.) and PTFE (Du Pont Co.) emulsion were mixed in distilled water with ultrasonic agitation. The mixture of the Pd/C and PTFE emulsion was pasted on carbon paper and then dried in an oven at 120 °C for 24 h in a stream of nitrogen gas. The pasted sheet was pressed with 2 MPa pressure. Finally, the Pd/C electrode with 15 mm dia. and 0.2 mm thickness, was obtained. The Pd/C electrode was wetted by dipping the specimen into 0.1 M NaOH for 24 h at room temperature. The

* Author to whom correspondence should be addressed.

0021-891X

wetted Pd/C electrode was used for cyclic voltammetry and a.c.-impedance measurements.

The aqueous solution of 0.1 M NaOH was deaerated by bubbling with purified nitrogen gas before and during the cyclic voltammetry and a.c.-impedance experiments. The geometrical surface area of the electrode exposed to electrolyte was 1.54 cm^2. A platinum wire and a saturated calomel electrode (SCE) were used as counter electrode and reference electrode, respectively. The potential of the reversible hydrogen electrode (RHE) was measured to be about −0.90 V vs SCE in the same solution. All potentials quoted in this work are referred to SCE.

Cyclic voltammograms were measured with the Pd/C, carbon and Pd foil electrodes in the potential range −1.50 to 1.00 V vs SCE at a scan rate of 100 mV s^{-1} using a potentiostat (EG&G PAR, model 273) interfaced with an IBM compatible computer.

The electrode impedance was measured using a frequency response analyser (Solartron, SI 1255 FRA) in conjunction with a potentiostat (EG&G PAR, model 273). A single sinusoidal potential wave of 10 mV peak-to-peak was superimposed on the constant potentials from −1.50 to −0.70 V vs SCE over the frequency range from 10^{-3} to 10^4 Hz. The frequency was scanned from high to low values.

All electrochemical experiments were carried out at room temperature.

3. Results and discussion

Typical cyclic voltammograms of the Pd/C, carbon and Pd foil electrodes in 0.1 M NaOH solution are presented in Fig. 1. In the voltammogram of the carbon electrode, no significant redox peak is observed over the potential range studied in this work, indicating a sluggish electrochemical reaction. The cathodic currents at the Pd/C electrode are much larger than those at the carbon electrode below −0.90 V vs SCE (~ 0 V vs RHE). The increased cathodic currents at the Pd/C electrode are probably due to the electrochemically active area produced by the dispersion of Pd. The electrochemically active area is approximately identical to the area of the dispersion of Pd because the h.e.r. proceeds dominantly on Pd rather than on carbon.

The electrochemically active surface area of the Pd/C electrode was evaluated quantitatively as follows. It is reported that Pd is entirely oxidized to Pd oxide at potentials above 0.50 V vs SCE. On the other hand, Pd oxide is completely reduced to Pd below −0.30 V vs SCE [9, 10]. Assuming that Pd oxide is composed of PdO or $Pd(OH)_2$, the amount of charge necessary for reduction of a monolayer of Pd oxide on a smooth Pd electrode was reported to be 255 $\mu C\,cm^{-2}$ [11]. From the present result of cyclic voltammetry the total charge for reduction of Pd oxides was calculated as 66.9 mC which means the dispersed Pd particles occupy an electrochemically active surface area of 262 cm^2. On the other hand, it is qualitatively expected from the sluggish electrochemical reaction that the powdered carbon electrode has a small electrochemically active area.

The voltammogram for the Pd/C electrode is qualitatively similar to that for the Pd foil, but the potentials corresponding to the current peaks are different. For positive going scans the Pd/C and Pd foil electrodes showed a broad peak at −0.50 and −0.20 V vs SCE, respectively. These peaks are related to the oxidation of hydrogen adsorbed on and absorbed in the electrode specimens. As the potential scan reverses, the cathodic current peaks corresponding to the decomposition of Pd oxide on the Pd/C and Pd foil electrodes occur at about −0.70 and −0.30 V vs SCE, respectively. The peaks of the hydrogen oxidation and of the Pd oxide reduction at the Pd/C electrode appeared in a more negative potential range than those at the Pd foil electrode.

Since the finely dispersed Pd particles have a higher specific active area than the smooth Pd foil specimen, it is reasonable to assume that most of the hydrogen atoms dwell adsorbed on the surface of the Pd/C electrode specimen, whereas they reside absorbed in the subsurface of the Pd foil electrode specimen. The

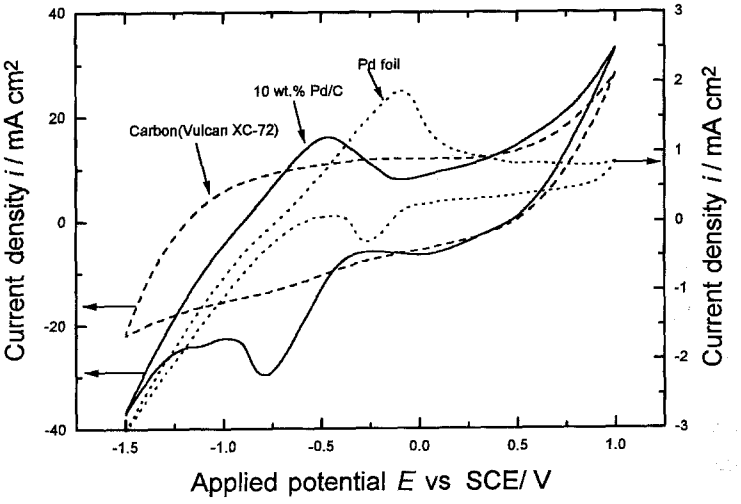

Fig. 1. Cyclic voltammograms in 0.1 M NaOH solution at a scan rate of 100 mV s^{-1} obtained for: 10 wt % palladium–dispersed carbon, (——); carbon (Vulcan XC-72), (– – – –); palladium foil, (· · · · ·).

hydrogen oxidation at the Pd/C electrode is entirely due to the desorption of hydrogen adsorbed on the surface of the finely dispersed Pd particles; however, oxidation at the Pd foil electrode proceeds by the desorption of hydrogen absorbed just beneath the electrode surface coupled with hydrogen diffusion through the Pd foil toward the surface [5, 7]. The shift of the hydrogen oxidation peak in the negative direction seems to be due to slow hydrogen diffusion through the Pd foil electrode.

Figures 2, 3 and 4 show Nyquist plots of the impedance spectra for the Pd/C, carbon and Pd foil electrodes in 0.1 M NaOH solution in the potential range −1.40 to −0.80 V vs SCE. The impedance spectra for the Pd/C and carbon electrodes are composed of one single semicircle over the whole frequency range. However, for the Pd foil electrode

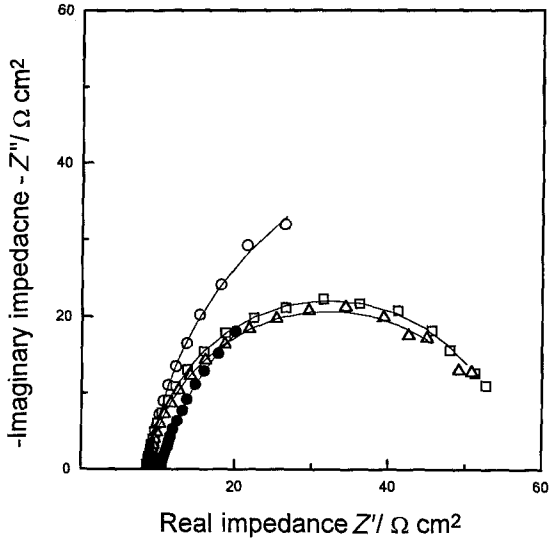

Fig. 2. Impedance spectra in the Nyquist presentation obtained for the 10 wt % palladium-dispersed carbon electrode in 0.1 M NaOH solution at potentials of −0.80 (○), −1.00 (□), −1.20 (△) and −1.40 (●) V vs SCE. Solid lines represent the simulated curves calculated with optimum fitted-parameters.

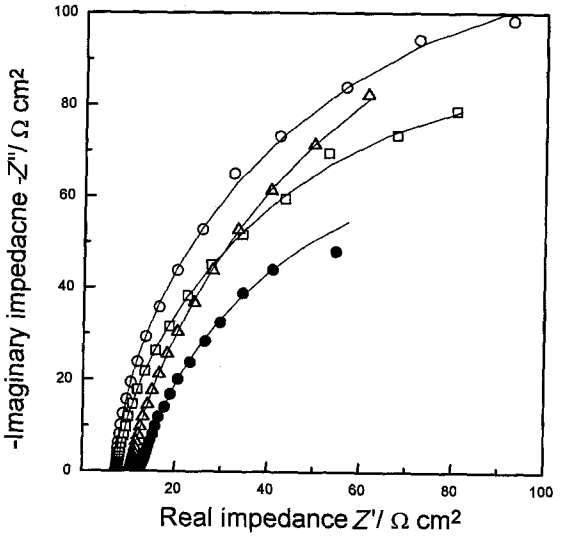

Fig. 3. Impedance spectra in the Nyquist presentation obtained for the carbon (Vulcan XC-72) electrode in 0.1 M NaOH solution at potentials of −0.80 (○), −1.00 (□), −1.20 (△) and −1.40 (●) V vs SCE. Solid lines represent the simulated curves calculated with optimum fitted-parameters.

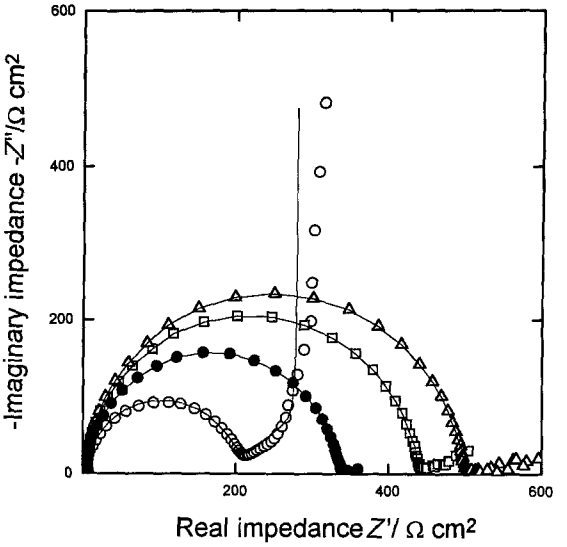

Fig. 4. Impedance spectra in the Nyquist presentation obtained for the palladium foil electrode in 0.1 M NaOH solution at potentials of −0.84 (○), −0.92 (□), −0.98 (△) and −1.02 (●) V vs SCE. Solid lines represent the simulated curves calculated with optimum fitted-parameters.

a Warburg impedance due to diffusion of hydrogen appears at −0.84 V vs SCE in the low frequency range. The Warburg impedance decreases at more negative potentials below −0.92 V vs SCE. This means that the rate-determining step is the h.e.r. at the Pd/C and carbon electrodes in the whole potential range and at the Pd foil electrode below −0.92 V vs SCE.

It is well established that the h.e.r. proceeds through three reaction steps, that is, the Volmer, Heyrovsky and Tafel reactions [1–3]. Disregarding the mass transport in the solution and electrode, the faradaic admittance Y_f for the h.e.r. is [2, 4]

$$Y_f = \frac{1}{Z_f} = A + \frac{B}{j\omega + C} = \frac{1}{R_{ct} + \left(j\omega C_{ad} + \frac{1}{R_{ev}}\right)^{-1}} \quad (1)$$

with $R_{ct} = 1/A$, $C_{ad} = -A^2/B$ and $R_{ev} = -B/A(AC + B)$. Z_f is the faradaic impedance; j, the imaginary number; ω, the angular frequency; R_{ct}, the charge transfer resistance; C_{ad}, the adsorption capacitance, and R_{ev}, the hydrogen evolution resistance. The kinetic parameters of A, B and C are defined as

$$A \equiv -F\left(\frac{\partial r_0}{\partial \eta}\right)_\theta, \quad B \equiv -\frac{F}{\Gamma_{max}}\left(\frac{\partial r_0}{\partial \theta}\right)_\eta \left(\frac{\partial r_1}{\partial \eta}\right)_\theta \text{ and}$$

$$C \equiv -\frac{1}{\Gamma_{max}}\left(\frac{\partial r_1}{\partial \theta}\right)_\eta$$

with $r_0 = v_1 + v_2$ and $r_1 = v_1 - v_2 - 2v_3$. v_1 is the Volmer reaction rate; v_2, the Heyrovsky reaction rate; v_3, the Tafel reaction rate; F, the Faraday constant; η, the overpotential; θ, the surface coverage, and Γ_{max}, the maximum surface concentration of adsorbed hydrogen. Hence, the total impedance Z_t for the h.e.r. is expressed as

$$Z_t = R_s + \frac{1}{(j\omega)^\varphi C_{dl} + Y_f} \quad (2)$$

where R_s is the solution resistance, φ is the depression parameter and C_{dl} is the double layer capacitance.

The measured impedance spectra were analysed using the faradaic admittance Y_f for the h.e.r. The real and imaginary components, Z' and $-Z''$, obtained at each applied d.c. potential were determined using the CNLS fitting method first written by Macdonald *et al.* [12] and modified in our laboratory [13] to determine such parameters involved in the faradaic admittance Equation 1, as C_{dl}, R_{ct} and R_{ev}. The calculation was performed with an IBM personal computer. Modulus weighting was selected as a weighting method in the CNLS fitting. The values of error for all the present fitting results were within 5%.

Figures 5 and 6 present the double layer capacitance C_{dl} and charge transfer resistance R_{ct}, respectively, for the h.e.r. on the Pd/C, Pd foil and carbon electrodes in 0.1 M NaOH solution as a function of the electrode potential. The Pd/C and carbon electrodes had an almost potential-independent value of $C_{dl} \approx 80\,\text{mF cm}^{-2}$. The Pd foil electrode had a much smaller, also potential-independent value of C_{dl}, $\sim 100\,\mu\text{F cm}^{-2}$. The comparatively high values of C_{dl} for the Pd/C and carbon electrodes indicate a porous character with a large real surface area. The charge transfer resistances R_{ct} for the h.e.r. on the Pd/C, carbon and Pd foil electrodes had maxima of 41, 252 and $520\,\Omega\text{cm}^2$ at -1.10, -1.20 and -0.96 V vs SCE, respectively.

A real surface area of the porous Pd/C and carbon electrodes of almost $4700\,\text{cm}^2$ is estimated from the experimental value $C_{dl} \approx 80\,\text{mF cm}^{-2}$ and the Helmholtz double layer capacitance value of $17\,\mu\text{F cm}^{-2}$ calculated theoretically at the metal/electrolyte interface [14]. The Pd foil electrode shows a real surface area of about $5.9\,\text{cm}^2$.

The values of R_{ct} for the Pd/C electrode are smaller than those values for the carbon electrode over the whole potential range. The smaller values of R_{ct} for Pd/C are presumably caused by the larger electrochemically active area than the carbon electrode in spite of almost the same value of the real surface area. From the potential dependence of the hydrogen coverage of the Pd foil electrode [7], it is inferred that the hydrogen coverage of the Pd/C electrode should also be affected by the potential. It is concluded that the maxima of R_{ct} for the Pd/C and Pd foil electrodes are due to the hydrogen coverage. Thus, the magnitude of the R_{ct} value for the Pd/C and carbon electrodes is determined by the electrochemically active surface area and the potential dependence of R_{ct} for the Pd/C and Pd foil electrodes is influenced by the hydrogen coverage.

Figure 7 illustrates the potential dependence of the hydrogen evolution resistance R_{ev} for the Pd/C and

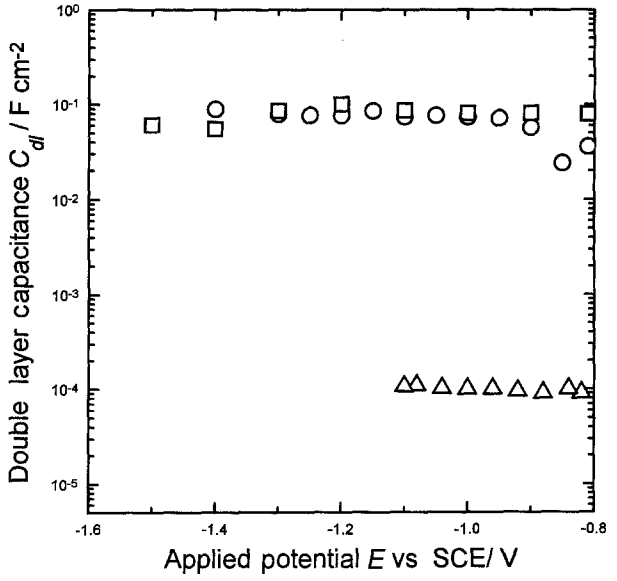

Fig. 5. Double layer capacitance C_{dl} against potential, calculated from impedance spectra of 10 wt % palladium–dispersed carbon electrode (○), carbon (Vulcan XC-72) electrode (□) and palladium foil electrode (△) in 0.1 M NaOH solution.

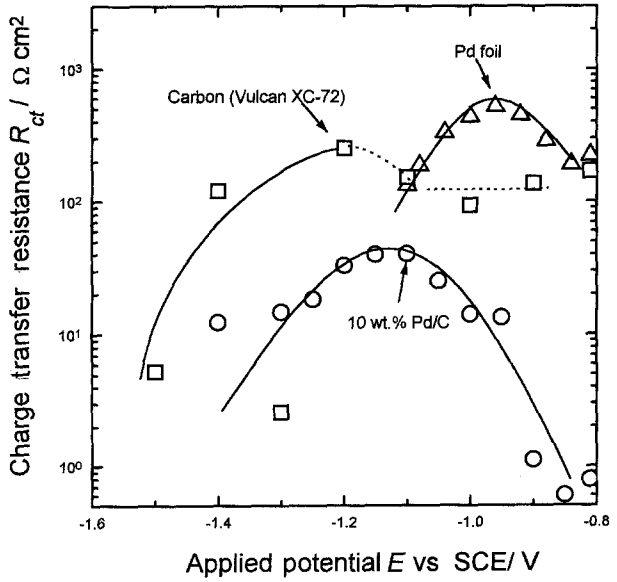

Fig. 6. Dependence of the charge transfer resistance R_{ct} on potential, calculated from impedance spectra of 10 wt % palladium–dispersed carbon electrode (○), carbon (Vulcan XC-72) electrode (□) and palladium foil electrode (△) in 0.1 M NaOH solution.

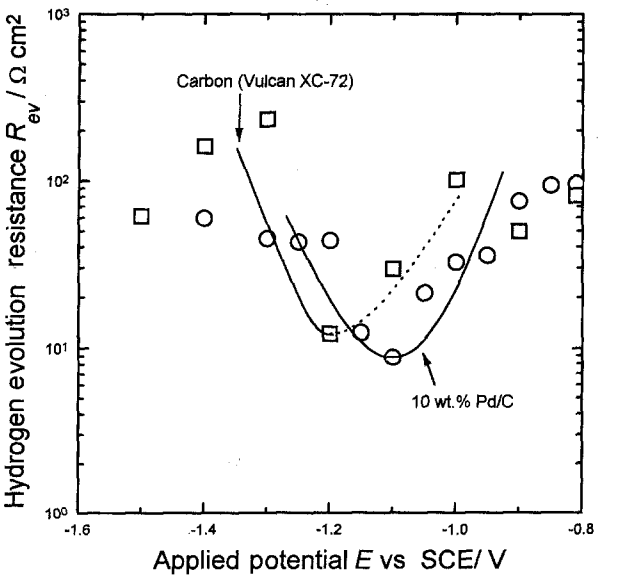

Fig. 7. Potential dependence of the hydrogen evolution resistance R_{ev} calculated from impedance spectra of 10 wt % palladium–dispersed carbon electrode (○) and carbon (Vulcan XC-72) electrode (□) in 0.1 M NaOH solution.

carbon electrodes in 0.1 M NaOH solution. The impedance spectra in the low frequency region involve the h.e.r. In the potential range below −0.92 V vs SCE, hydrogen bubbles evolved from the Pd electrode disturb the current response to the sinusoidal potential wave. Thus, the impedance spectra become so scattered that R_{ev} cannot be obtained. The R_{ev} for the Pd/C and carbon electrodes have minima at −1.10 and −1.20 V vs SCE, respectively. The maximum R_{ct} and minimum R_{ev} for the Pd/C and carbon electrodes occur at the same potential. The occurrence of the minimum R_{ev} means that the h.e.r. at the Pd/C and carbon electrodes takes place intensively below −1.10 V vs SCE and −1.20 V vs SCE, respectively, and that at both the electrodes it does so very slowly above these potentials. Hydrogen absorption and diffusion in the carbon electrode proceeds sluggishly over the whole potential range. Therefore, the values of R_{ct} and R_{ev} for the h.e.r. at the carbon electrode are physically meaningless above −1.20 V vs SCE. From the high solubility of hydrogen in Pd, it is suggested that the h.e.r. at the Pd/C electrode takes place simultaneously with hydrogen absorption and diffusion above −1.10 V vs SCE, whereas the former dominates over the latter below −1.10 V vs SCE. On the other hand, the h.e.r. at the Pd foil electrode does the same above and below −0.96 V vs SCE.

The hydrogen evolution overpotentials referred to the reversible potential of the hydrogen electrode at about −0.90 V vs SCE. The hydrogen evolution overpotential for the Pd/C electrode is lower by 0.1 V than that of the carbon electrode. This is due to the effect of the electrochemically active surface area increased by the finely dispersed Pd particles. On the other hand, the hydrogen evolution overpotential at the Pd/C electrode is higher by 0.14 V than that on the Pd foil electrode. This can be accounted for in terms of two competing contributions to the h.e.r. The positive contribution of the finely dispersed Pd particles to the h.e.r. is exceeded by the negative contribution of the carbon to the h.e.r. at which the hydrogen evolution rate is very sluggish. Thus, this raises the hydrogen evolution overpotential.

Measurements of the a.c.-impedance were also carried out with the 20 wt % Pd/C electrode. The impedance spectra were so scattered at potentials below −1.00 V vs SCE that they cannot be analysed. The current response to a sinusoidal potential wave is disturbed by hydrogen bubbles evolved from the finely dispersed Pd particles. The h.e.r. on the 20 wt % Pd/C electrode takes place vigorously below −1.00 V vs SCE. Potentiodynamic polarization measurements were carried out with the 10 wt % and 20 wt % Pd/C electrodes in 0.1 M NaOH solution. Below −1.10 V vs SCE, the cathodic branch of the polarization curves on the Pd/C electrode specimens does not obey Tafel's law, but it is characterized by the appearance of the limiting hydrogen diffusion current. In contrast, the platinum–dispersed carbon (Pt/C) and nickel-containing glass-metal electrodes both have a relatively small cathodic Tafel slope of about 30 mV decade^{-1} [15]. The electrochemical activity of the Pd/C electrode in this work is inferior to Pt/C and nickel alloy electrodes.

The electrochemical activity for the h.e.r. of the Pd/C electrode could be improved to some extent by accurately controlling the amount and extent of the Pd dispersion in the electrode. Based on the results of this work, further work on the h.e.r. on Pd powder specimens as a positive catalyst and hydride forming metal specimen as a negative catalyst will explore the particle size and dispersion grade for practical applications in hydrogen production and nickel/metal hydride secondary batteries.

4. Conclusions

The analysis of the a.c.-impedance spectra showed maximum charge transfer resistances R_{ct} and minimum hydrogen evolution resistances R_{ev} for the h.e.r. approximately at the same electrode potential for the Pd/C, carbon and Pd foil electrodes, respectively. From the experimental results the conclusions are: (i) the h.e.r. proceeds markedly at the Pd/C electrode along with the absorption and diffusion of hydrogen into the electrode above −1.10 V vs SCE, whereas that h.e.r. becomes faster than absorption and diffusion below −1.10 V vs SCE. The Pd foil electrode showed transition from absorption and diffusion to evolution at −0.96 V vs SCE; (ii) the h.e.r. rate at the carbon electrode is higher than 1 mA cm^{-2} below −1.20 V vs SCE. The charge transfer resistance R_{ct} and the hydrogen evolution overpotential at the Pd/C electrode are lower than at the carbon electrode owing to the electrochemically active area caused by the finely dispersed Pd particles.

Acknowledgements

This work was financially supported in part by the Ministry of Science and Technology, and Ministry of Commerce and Industry, Korea, under the program 'Development of Fuel Cell Technology, 1993'. The authors are grateful to Y.-G. Ryu, Department of Materials Science & Engineering, KAIST, for many helpful suggestions and discussions.

References

[1] J. O'M. Bockris and A. K. N. Reddy, 'Modern Electrochemistry', Vol. 2, Plenum, New York (1970) pp. 1141–51.
[2] L. Bai, D. A. Harrington and B. E. Conway, *Electrochim. Acta* **32** (1987) 1713.
[3] M. Enyo, *in* 'Comprehensive Treatise of Electrochemistry', Vol. 7 (edited by J. O'M. Bockris, E. Yeager, S. V. M. Khan and R. E. White), Plenum Press, New York, (1988) p. 241.
[4] E. Endoh, H. Otouma, T. Morimoto and Y. Oda, *Int. J. Hydrogen Energy* **12** (1987) 473.
[5] J. Fournier, P. W. Wrona, A. Lasia, R. Lacasse, J.-M. Lanacette, H. Menard and L. Brossard, *J. Electrochem. Soc.* **139** (1992) 2372.

[6] V. Breger and E. Gileadi, *Electrochim. Acta* **16** (1971) 177.
[7] C. Lim and S.-I. Pyun, *ibid.* **39** (1994) 363.
[8] T. H. Yang and S.-I. Pyun, *Electrochim. Acta* (1996) in press.
[9] N. Tateishi, K. Yahikozawa, K. Nishimura, M. Suzuki, Y. Iwanaga, M. Watanabe, E. Eunami, Y. Matsuda and Y. Takasu, *ibid.* **36** (1991) 1235.
[10] J.-D. Kim, S.-I. Pyun, T.-H. Yang and J.-B. Ju, *J. Electroanal. Chem.* **383** (1995) 161.
[11] F. G. Will and C. A. Knorr, *Z. Elektrochem.* **64** (1960) 258.
[12] J. R. Macdonald, 'Impedance Spectroscopy', J. Wiley & Sons, New York (1987) p. 16.
[13] J.-S. Bae and S.-I. Pyun, *J. Mat. Sci. Lett.* **13** (1994) 573.
[14] J. O'M. Bockris and A. K. N. Reddy, 'Modern Electrochemistry', Vol. 2, Plenum, New York (1970) pp. 741–61.
[15] J. Vracar and B. E. Conway, *J. Electroanal. Chem.* **277** (1990) 253.